

## Article

# Spatial and Temporal Variability of Extreme Hydroclimatic Events in the Bani River Basin

Fousseini Kouyaté<sup>1,2,\*</sup> , François Kossi Guédjé<sup>1,3,\*</sup>, Assane Ndiaye<sup>1,2</sup> and Orou Moctar Ganni Mampo<sup>1,2</sup>

<sup>1</sup> Graduate Research Program on Climate Change and Water Resources, West African Science Service Center on Climate Change and Adapted Land Use (WASCAL), University of Abomey-Calavi, Abomey-Calavi BP 2008, Benin

<sup>2</sup> Laboratory of Applied Hydrology, University of Abomey-Calavi, Abomey-Calavi BP 2008, Benin

<sup>3</sup> Laboratory of Atmospheric Physics (LPA), Department of Physics, Faculty of Science and Technology, University of Abomey-Calavi, Abomey-Calavi BP 2008, Benin

\* Correspondence: kouyate.f@edu.wascal.org (F.K.); guedjefranco@yahoo.com (F.K.G.);  
Tel.: +223-74684174 (F.K.); +229-97487642 (F.K.G.)

**Abstract:** Severe hydroclimatic events affect ecosystems and human livelihoods, creating significant challenges for managing water resources. This study analyzed the rainfall and river flow trends in the Bani River Basin (BRB) from 1991 to 2020. Using indices such as the maximum rainfall over a one-day period (RX1DAY), maximum rainfall over a five-day period (RX5DAY), rainfall exceeding the 95th percentile (R95P), simple daily precipitation intensity (SDII), and peak discharge (Qmax), the modified Mann–Kendall test and Pettitt’s test were applied to assess the trends and identify potential breakpoints. The results revealed spatial variability, with southern regions showing reduced rainfall, while northeastern areas exhibit increasing extreme rainfall and river flow. The RX5DAY declined significantly after 2000, reflecting reductions in prolonged rainfall events, followed by the RX1DAY, which declined significantly after 2012, indicating a reduction in short-duration extremes. In contrast, the R99P, SDII, and Qmax exhibited positive trends, indicating intensifying rainfall intensity and extremes in discharge. A notable breakpoint was detected in 1993, marking a transition to increased extreme flows. The highest values of the rainfall indices (R95P, R99P, RX1DAY, RX5DAY, SDII) were concentrated in the southern part of the basin, while the north recorded lower values. These results highlight the basin’s vulnerability to climate variability and provide insights into hydroclimatic changes, serving as a basis for informed decision-making and future research.

**Keywords:** hydroclimatic variability; Bani River Basin; rainfall; river flow trends; extreme rainfall indices



Academic Editor: Yanfang Sang

Received: 4 December 2024

Revised: 29 December 2024

Accepted: 31 December 2024

Published: 5 January 2025

**Citation:** Kouyaté, F.; Guédjé, F.K.; Ndiaye, A.; Ganni Mampo, O.M. Spatial and Temporal Variability of Extreme Hydroclimatic Events in the Bani River Basin. *Hydrology* **2025**, *12*, 5. <https://doi.org/10.3390/hydrology12010005>

**Copyright:** © 2025 by the authors. Licensee MDPI, Basel, Switzerland. This article is an open access article distributed under the terms and conditions of the Creative Commons Attribution (CC BY) license (<https://creativecommons.org/licenses/by/4.0/>).

## 1. Introduction

West Africa faces growing challenges related to climate variability and human-induced changes, which significantly impact its river systems. Among these challenges are alterations in rainfall patterns and river flows, driven by factors such as dam construction, land-use changes, and global climate change [1,2]. These dynamics are particularly critical in regions where water resources play a central role in sustaining agriculture, fisheries, and livelihoods for millions of people [3]. While research on West Africa’s river systems has primarily focused on larger and better-documented basins such as the Senegal and Niger, the Bani River Basin has received comparatively less attention, despite its critical role as a tributary of the Niger River and its unique hydrological vulnerabilities [4]. Understanding and quantifying these trends is crucial for ensuring sustainable water resource management

and mitigating the effects of hydrological extremes [5]. The hydroclimatic variability in West Africa has been extensively documented, with research highlighting significant temporal and spatial changes in rainfall and river flow across the region. Studies have reported an increase in extreme rainfall events and river discharge in the Senegal River Basin, with a notable shift to wetter conditions [6]. Significant transitions in annual rainfall patterns have also been identified, with periods of drought followed by partial recovery after 1994 [7]. These findings align with broader studies demonstrating the sensitivity of river basins like the Bani to both natural climate cycles and anthropogenic influences [8,9]. However, the Bani River Basin (BRB) faces specific challenges due to its semi-arid environment, reliance on rain-fed agriculture, and significant human pressures from land-use changes and water infrastructure development. Unlike larger basins, it lacks the extensive monitoring and data resources necessary for understanding its hydrological behavior, making this study particularly important [10]. Additionally, the interplay between rainfall variability and dam construction has revealed significant alterations in hydrological regimes that are likely mirrored in the Bani Basin [11]. Together, these studies underscore the complex drivers of hydrological change across West Africa, including climatic and human-induced factors.

The BRB itself has been the subject of targeted research, emphasizing its unique hydrological characteristics and vulnerabilities. Hydrological models have been used to assess the basin's response to rainfall variability, identifying substantial impacts on river flow and water resource availability [8]. The intricate interactions between surface water and groundwater in the basin have provided critical insights into its hydrological processes [9]. These findings are complemented by simulations of the hydrological dynamics under varying climatic and land-use scenarios, which highlight the basin's susceptibility to environmental changes [12]. This study also contributes to addressing these knowledge gaps by focusing specifically on the rainfall and river flow trends in the Bani Basin, leveraging statistical methods that provide a detailed temporal analysis. Such an approach offers a more nuanced understanding of its hydroclimatic variability compared to existing regional studies [13]. Additionally, climate change projections for river flows across West Africa emphasize the heightened vulnerabilities of semi-arid regions like the Bani River Basin [14].

The challenges faced by the BRB are not unique but are indicative of broader trends across West African river basins. Recent works demonstrate the interconnection between regional climate patterns, anthropogenic interventions, and hydrological responses [6,11]. For example, the construction of dams has been shown to significantly modify flow regimes and sediment transport, which are key concerns in the BRB. Furthermore, long-term studies on rainfall trends provide a foundation for understanding the basin's hydrological variability [3,8].

Despite these advances, the BRB remains less studied than major basins like the Senegal and Niger. This work is novel in its comprehensive approach to assessing both natural and anthropogenic factors driving hydrological change in the Bani River Basin. Unlike previous studies, which have largely focused on regional-scale impacts, this research integrates local-scale hydrological data and statistical techniques to uncover trends and transitions specific to the BRB [15]. This study aims to fill this gap by conducting a comprehensive assessment of the trends and significant changes in rainfall and river flow within the BRB. By integrating historical observations and statistical techniques, this research seeks to provide a deeper understanding of the basin's hydroclimatic dynamics. The outcomes will not only contribute to scientific knowledge but also inform sustainable water resource management and adaptation strategies, addressing the challenges posed by climate variability and human interventions in the region.

## 2. Materials and Methods

### 2.1. Study Area

The Bani River, the largest tributary of the Upper Niger River, is primarily situated in Mali, with portions extending into Côte d'Ivoire and Burkina Faso. Its catchment area covers approximately 129,400 km<sup>2</sup>, as measured at the Mopti gauging station (Figure 1). This basin was chosen for this study due to its high-quality hydrological and climatic data compared to other regional basins, making it ideal for studies. Moreover, the absence of major hydraulic infrastructure in the BRB ensures that the river's natural flow regime is largely preserved, facilitating the accurate assessment of hydrological processes [12,16]. The topography of the basin is characterized by a gradual slope, with elevations ranging from 852 m in the south and central-eastern areas to 217 m at the northern outlet. The Bani catchment falls in the Sudano-Sahelian climatic zone, and the river flows from south to north along a pronounced precipitation gradient. The annual rainfall varies significantly across the basin, from approximately 1250 mm in the southern regions to about 615 mm in the northern areas [16].

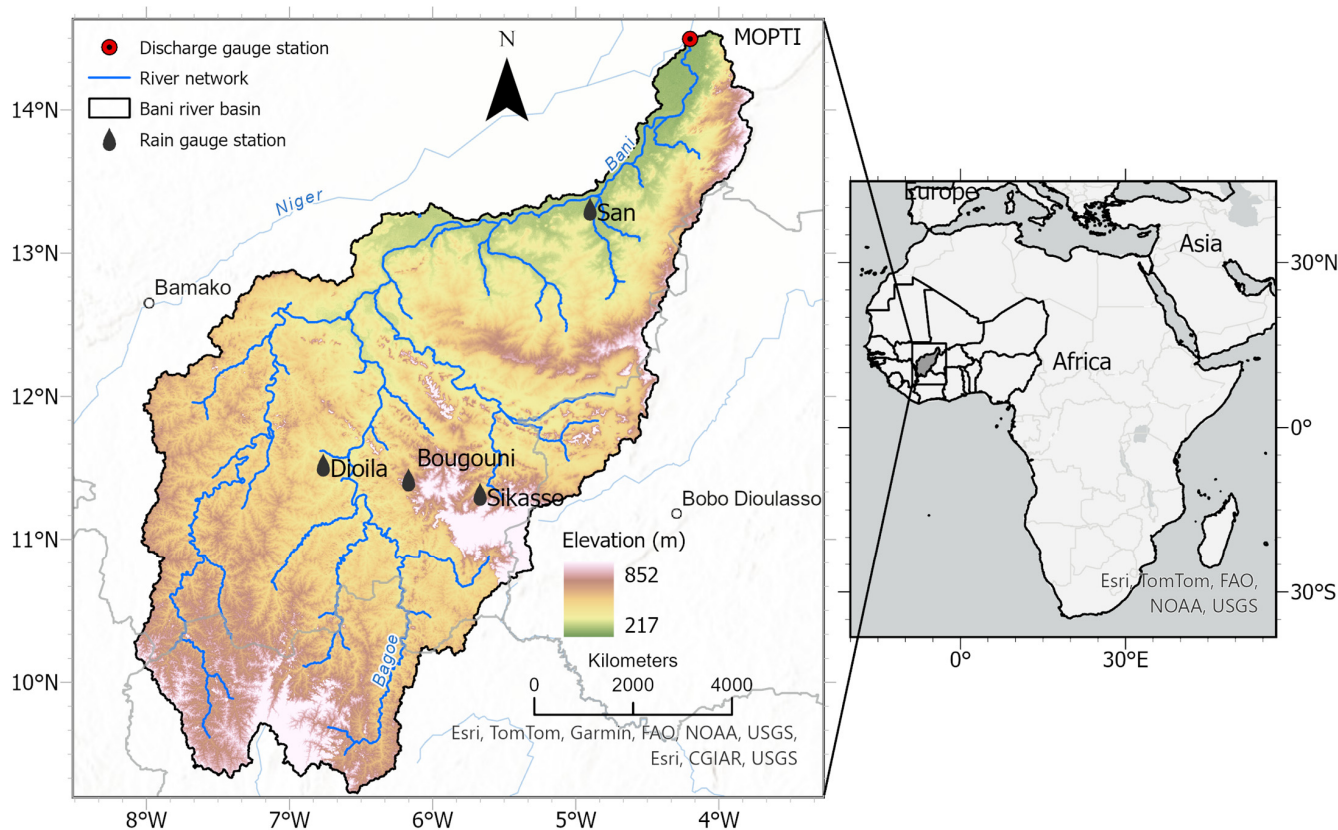


**Figure 1.** Location of the Bani River Basin.

### 2.2. Data

This study analyzes 30 years of data (1991–2020) for the Bani River Basin. Precipitation data were sourced from the CHIRPS dataset (<https://iridl.ldeo.columbia.edu/SOURCES/.UCSB/.CHIRPS/.v2p0/.daily/.global/.0p05/> (accessed on 12 February 2023)), known for its high resolution (0.05°) and validated reliability for West Africa [17]. CHIRPS effectively captures the rainfall variability across diverse climatic zones, making it suitable for hydrological modeling. The observed rainfall from 2011 to 2019 was collected from Agence Nationale de la Météorologie du Mali. Discharge data were obtained from the Mopti station, the basin's outlet, provided by the Direction Nationale de l'Hydraulique du Mali. This station's records reflect the natural flow regime, as the basin remains free

from significant hydraulic infrastructure. These datasets enable robust analysis of the hydrological dynamics in the study area.

### 2.3. Methods

#### 2.3.1. Assessment of Observed and CHIRPS Rainfall Data

Between 2011 and 2019, the quality of the CHIRPS data was assessed by comparing it with rainfall measurements from four stations located along the BRB (Figure 1). Monthly variations in the satellite estimates were examined alongside the station records. The statistical indicator employed to evaluate the accuracy of CHIRPS was the Nash–Sutcliffe efficiency (NSE).

$$\text{NSE} = 1 - \frac{\sum(\text{Pr}_1 - \text{Pr}_2)^2}{\sum(\text{Pr}_1 - \overline{\text{Pr}_2})^2} \quad (1)$$

$\text{Pr}_1$  corresponds to the station-measured rainfall,  $\text{Pr}_2$  corresponds to the satellite-derived rainfall, and  $\overline{\text{Pr}_2}$  is the mean rainfall from the satellite data. The NSE ranges from negative infinity to 1; an NSE of 1 indicates perfect agreement between the satellite estimates and station data, while an NSE of 0 suggests that using CHIRPS yields about the same performance as simply taking the average observed value.

#### 2.3.2. Overview of Selected Extreme Rainfall and River Flow Indices

The rainfall and river discharge extremes were examined from 1991 to 2021 using specific indices to capture their variability and intensity. The rainfall indices included the extremely wet days (R99P), very wet days (R95P), simple daily intensity (SDII), maximum 1-day rainfall (RX1DAY) and maximum 5-day rainfall (RX5DAY), as shown in Table 1. For the river discharge, three indices were used to describe extreme flow conditions: peak flow ( $Q_{\max}$ ), high-flow days (Q95P), and very-high-flow days (Q99P). These metrics, calculated over the same period, are crucial for understanding hydrological dynamics during floods and droughts [6,18]. Additionally, the standardized flow index (SFI) was computed to assess the annual flow variations, identifying years of surplus or deficit. The standardized flow index is defined mathematically as:

$$I_i = \frac{Q_i - \overline{Q}}{\sigma} \quad (2)$$

**Table 1.** Classification of drought and wet conditions using the standardized flow index.

Values	Class
$I_i \geq 2$	Extremely wet
$1.5 \leq I_i \leq 1.99$	Very wet
$1.0 \leq I_i \leq 1.49$	Moderately wet
$-0.99 \leq I_i \leq 0.99$	Close to normal
$-1.0 \leq I_i \leq -1.49$	Moderately dry
$-1.5 \leq I_i \leq -1.99$	Very dry
$I_i \leq -2$	Extremely dry

$I_i$  is the standardized flow index,  $Q_i$  is the annual flow of a particular year, and  $\overline{Q}$  is the annual flow average over the period;  $\sigma$  is the standard deviation during the time.

The indices outlined in Table 2 offer critical insights into the extreme rainfall and river flow patterns. These indicators are vital for evaluating flood risks, improving water resource management, and understanding the hydrological dynamics of rivers in the region. Such analyses are indispensable for detecting trends in extreme events, supporting effective decision-making and planning to address climate variability and its effects on water resources.

**Table 2.** Indices for extreme rainfall and river flow.

Index	Name of the Index	Index Description	Units
SDII	Simple daily rainfall index	Ratio of yearly total rainfall to the number of rainy days	mm/day
RX1DAY	Max 1-day rainfall	Highest single-day rainfall total recorded within a year	mm
RX5DAY	Max 5-day rainfall	Highest total rainfall over any 5 consecutive days in a year	mm
R95P	Very wet days	Total yearly rainfall exceeding the 95th percentile (1991–2020)	mm
R99P	Extremely wet day	Total yearly rainfall exceeding the 99th percentile (1991–2020)	mm
Qmax	Peak discharge	Highest yearly river discharge (1991–2020)	m <sup>3</sup> /s
Q95P	High-flow days	Total yearly streamflow from days exceeding the 95th percentile (1991–2020)	m <sup>3</sup> /s
Q99P	Very-high-flow days	Total yearly streamflow from days exceeding the 99th percentile (1991–2020)	m <sup>3</sup> /s

### 2.3.3. Trend and Change-Point Detection

#### Tests for Trend Analysis

This study utilized the modified Mann–Kendall (MMK) test to examine the spatial and interannual trends in extreme rainfall and river flow across the BRB and its upper catchment during the period 1991–2020. The MMK test, a widely recognized nonparametric approach, was chosen for its suitability in analyzing the 30-year data series. It is particularly effective for hydrological and climatic datasets due to its minimal reliance on assumptions about the data distribution [6,19,20]. The use of MMK instead of the traditional Mann–Kendall (MK) test is justified by the presence of autocorrelation in the time series data, which violates the independence assumption of the MK test. As highlighted in [21], autocorrelation can significantly impact trend detection, with positive autocorrelation artificially inflating the significance of trends and negative autocorrelation masking actual trends.

An enhancement of the traditional Mann–Kendall (MK) test, the MMK method addresses the issue of autocorrelation in time series data, which can distort trend detection. Positive autocorrelation can exaggerate trend estimates, while negative autocorrelation can mask actual trends [19]. By adjusting the variance of the MK statistic to account for autocorrelation, the MMK test minimizes the likelihood of false trend detection [22]. The preprocessing steps involved in applying the MMK test, such as removing seasonal patterns, were necessary to isolate long-term trends from periodic fluctuations. However, these adjustments can affect the statistical significance of indices sensitive to short-term variability, such as the R95P [23].

The MMK test functions similarly to the classical MK test but incorporates adjustments to the variance of the test statistic ( $S$ ) to account for autocorrelation effects. This makes it particularly effective for datasets with complexities such as tied values, seasonality, or missing data. Although robust, the MMK test requires additional preprocessing steps, including addressing tied values and seasonal patterns, which add complexity to its implementation [20,24]. It has been demonstrated that methods accounting for persistence in time series, such as MMK, are crucial for ensuring reliable trend detection in data prone to autocorrelation [25].

$$\text{Var}(s) = \frac{1}{18} (n(n-1)(2n+5)) \frac{n}{ns^*} \quad (3)$$

The parameter  $ns^*$  is utilized to correct the effective number of observations, considering the autocorrelation in the data.

$$\frac{n}{ns^*} = 1 + \frac{2}{n(n-1)(n-2)} \sum_{s=1}^m (n-s) \quad (4)$$

$\frac{n}{ns^*}$  is a correction factor due to the autocorrelation present in the data.

The trend analysis was conducted using the “modifiedmk” package within the R programming environment, which is specifically designed to apply the modified Mann–Kendall (MMK) test while accounting for autocorrelation in time series data. This test evaluates the null hypothesis (H0) of “no trend” against the alternative hypothesis (H1) indicating the presence of a trend. A 5% significance level was employed to determine the statistical significance of the identified trends, aligning with common practices in hydrological and climatic research [26].

#### Change-Point Detection Tests

Pettitt’s test, a nonparametric method introduced in [27], is widely used to detect abrupt changes in time series data, such as shifts in climate or hydrological records. This test identifies statistically significant changes in the mean of a dataset by evaluating the null hypothesis (H0) of uniformity against the alternative hypothesis (H1) that a change has occurred. A change point is deemed statistically significant if the  $p$ -value is  $\leq 0.05$ . Pettitt’s test has been extensively applied in studies to analyze shifts in climatic and hydrological conditions [27,28].

The standard normal homogeneity test (SNHT) is a robust statistical tool for detecting discontinuities in time series, particularly at the beginning or end of a dataset. It is effective even with missing values, making it reliable for climatic and hydrological studies. The test’s strength lies in its ability to identify structural breaks in the data through its sensitivity and straightforward implementation. The application of the SNHT relies on the utilization of the following equation:

$$Q_i = Y_i - \frac{\sum_{j=1}^k \rho_j^2 X_{ij} \bar{y}}{\sum_{j=1}^k \rho_j^2} \quad 1 \leq i \leq n \text{ and } i \leq j \leq k \quad (5)$$

The base series comprises values denoted as  $Y_i$  for each year  $i$ , while the reference series, labeled  $j$ , contains observations represented as  $X_{ij}$  for each year  $i$ . The value  $\rho_j$  denotes the correlation coefficient between the base series and the reference series  $j$ .

These tests, the MMK, Pettitt’s test, and the SNHT, as shown in Figure 2, are valuable tools for trend detection and the identification of structural changes. However, their effectiveness and relevance depend on the specific characteristics of the analyzed data.

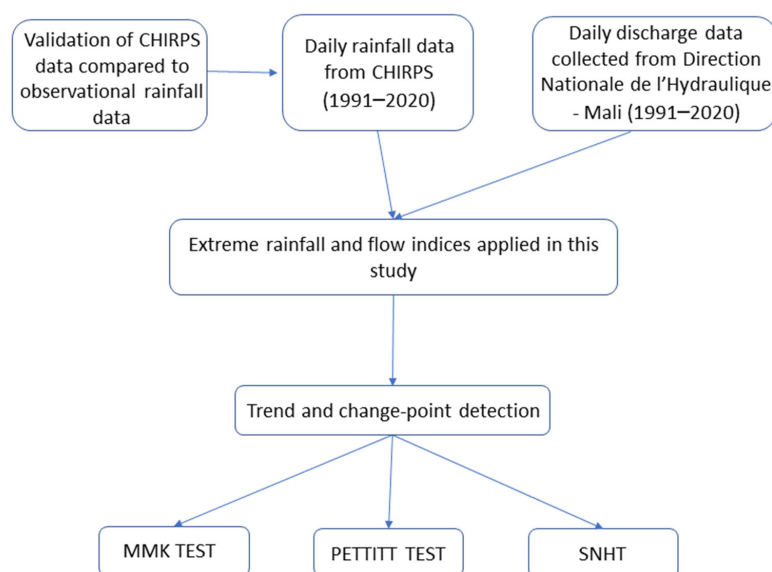


**Figure 2.** Flowchart illustrating the methodology applied.

### 3. Results

#### 3.1. Assessment of CHIRPS Data Quality

The NSE values presented in this study (Figure 3), ranging from 0.95 to 0.98, underscore the strong agreement between the CHIRPS satellite-based rainfall estimates and the ground-based station observations across the four locations (Figure 1). These high NSE values validate CHIRPS as a reliable tool for accurately estimating rainfall in the BRB region.

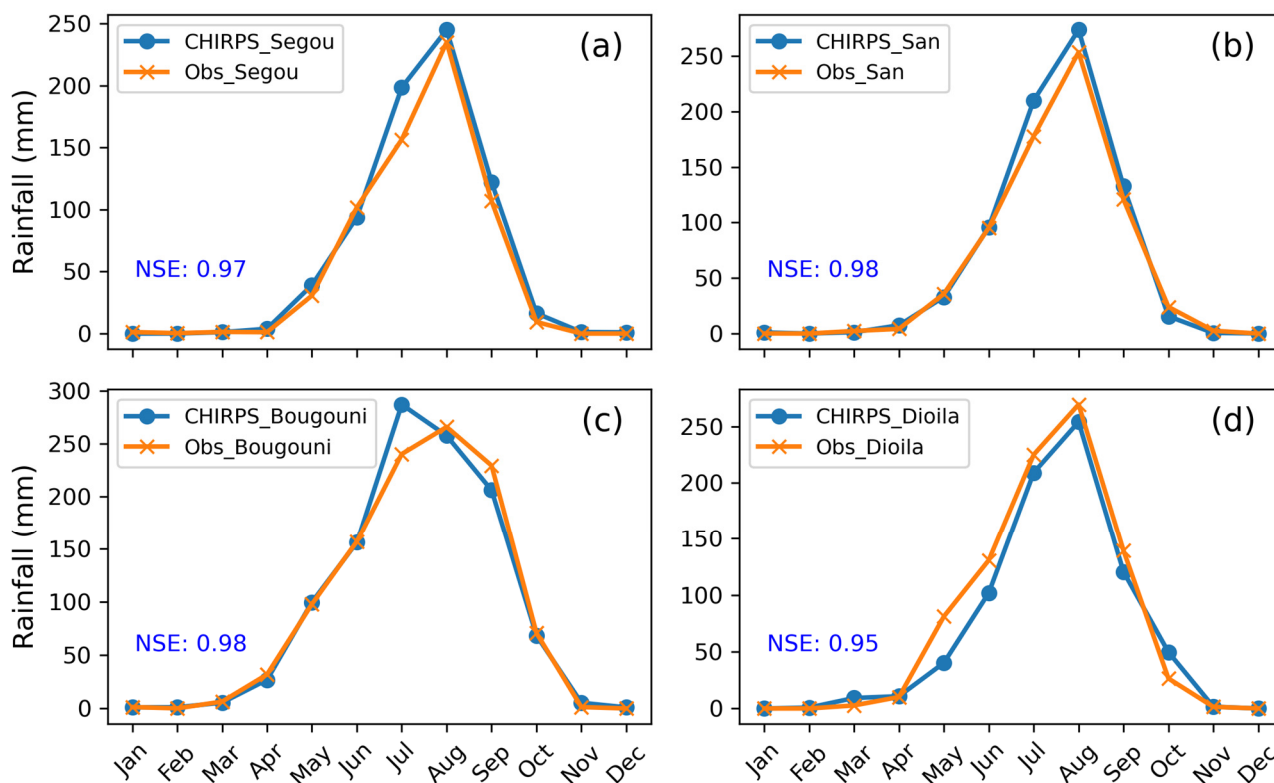


**Figure 3.** Monthly rainfall comparison between CHIRPS data and observed station measurements in the BRB (2011–2019): (a) Segou, (b) San, (c) Bougouni and (d) Dioila.

The observed trends in Figure 3a–d demonstrate that CHIRPS effectively captures the temporal and seasonal rainfall dynamics, particularly during the rainy season (June to September). Minor discrepancies in some months, such as the peak rainfall periods in Figure 3d, are minimal and fall within the acceptable limits for satellite-based estimations. These findings align with prior research. For instance, ref. [29] highlighted that CHIRPS is a dependable dataset for monitoring rainfall, particularly in regions with sparse observational networks. Similarly, ref. [10] validated CHIRPS in West Africa, demonstrating strong correlations with station data, making it highly suitable for agricultural planning.

#### 3.2. Spatial Variation in Extreme Rainfall Indices over the BRB

Figure 4 illustrates the spatial variation of the extreme rainfall indices, the RX1DAY, RX5DAY, R95P, R99P and SDII, for the period 1991–2020 during the rainy season (June to September) across the study area. Higher values of these indices are concentrated in the southern regions, with a maxima of approximately 10 mm/day for the SDII, 54 mm for the RX1DAY, 96 mm for the RX5DAY, 20 mm for the R95P, and 36 mm for the R99P. These patterns highlight a higher intensity and frequency of extreme rainfall in the southern part of the basin, while the lower values in the northern regions reflect reduced exposure to extreme rainfall events upstream. The coordinate system used for this spatial analysis

is the WGS84 geographic coordinate system, ensuring accurate and reproducible spatial representation.

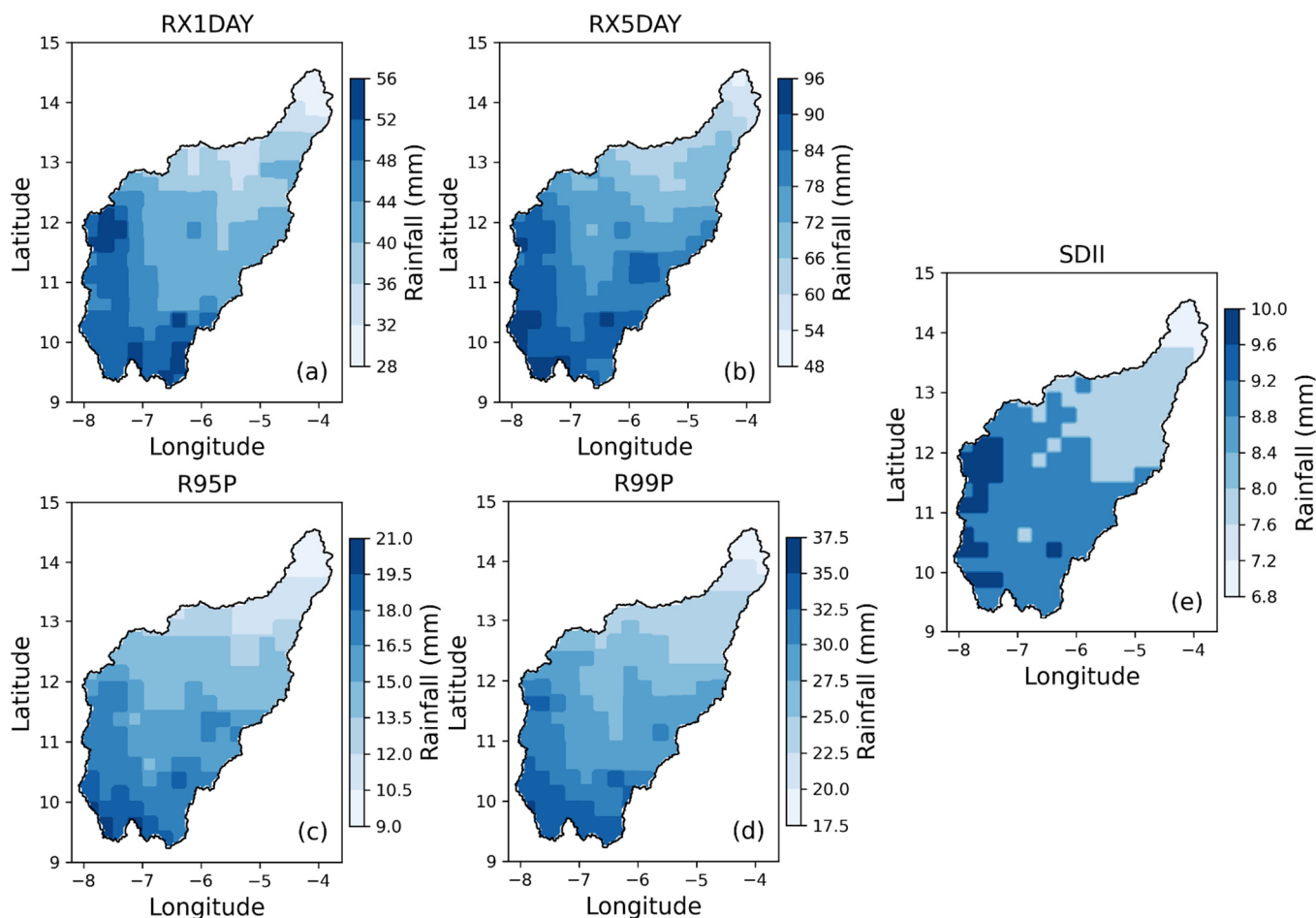


**Figure 4.** Spatial distribution of extreme rainfall indices across the study area (1991–2020): (a) maximum one-day precipitation, (b) maximum five-day precipitation, (c) very wet day, (d) extremely wet day, and (e) simple daily precipitation.

Such spatial disparities align with findings from across West Africa. For instance, ref. [17] reported increasing trends in extreme rainfall and the multi-day maxima in Benin, while ref. [30] highlighted a significant rise in the RX1DAY and cumulative rainfall in Nigeria. Similarly, ref. [6] observed a marked amplification of extreme rainfall events, particularly the RX5DAY and R95P, in the Senegal River Basin, consistent with broader trends across southern West Africa.

### 3.3. Trend and Significance of Extreme Indices

The spatial analysis of the Sen's slope trends in Figure 5 reveals notable variability across the study area in the extreme rainfall indices. The RX1DAY index in panel (a) highlights a positive and significant trend of the maximum one-day rainfall in the northern and northeastern regions, indicated by black dots ( $p < 0.05$ ). The RX5DAY index in panel (b) shows a significant upward trend in the five-day maximum precipitation in the northeastern and central regions, with a notable concentration of significant increases, while southern areas exhibit decreasing trends of lesser magnitude. Conversely, decreasing trends are observed in the southern part of the basin, with moderate significance. For the R99P index in panel (d), an increasing trend and significant rise in extremely wet days are concentrated in the northeastern areas. However, declining trends dominate the southwestern regions, indicating a reduction in extreme rainfall occurrences. The R95P index in panel (c) shows

a positive and significant trend of very wet days in the northeastern part of the basin, while the southern regions exhibit moderate to negative trends. The SDII index in panel (e) displays an upward trend in the daily rainfall intensity in the central and northeastern zones, with significant increases near the basin's center. In contrast, the southern areas reveal moderate or no meaningful changes in the rainfall intensity. This variation suggests uneven rainfall intensification across the basin.

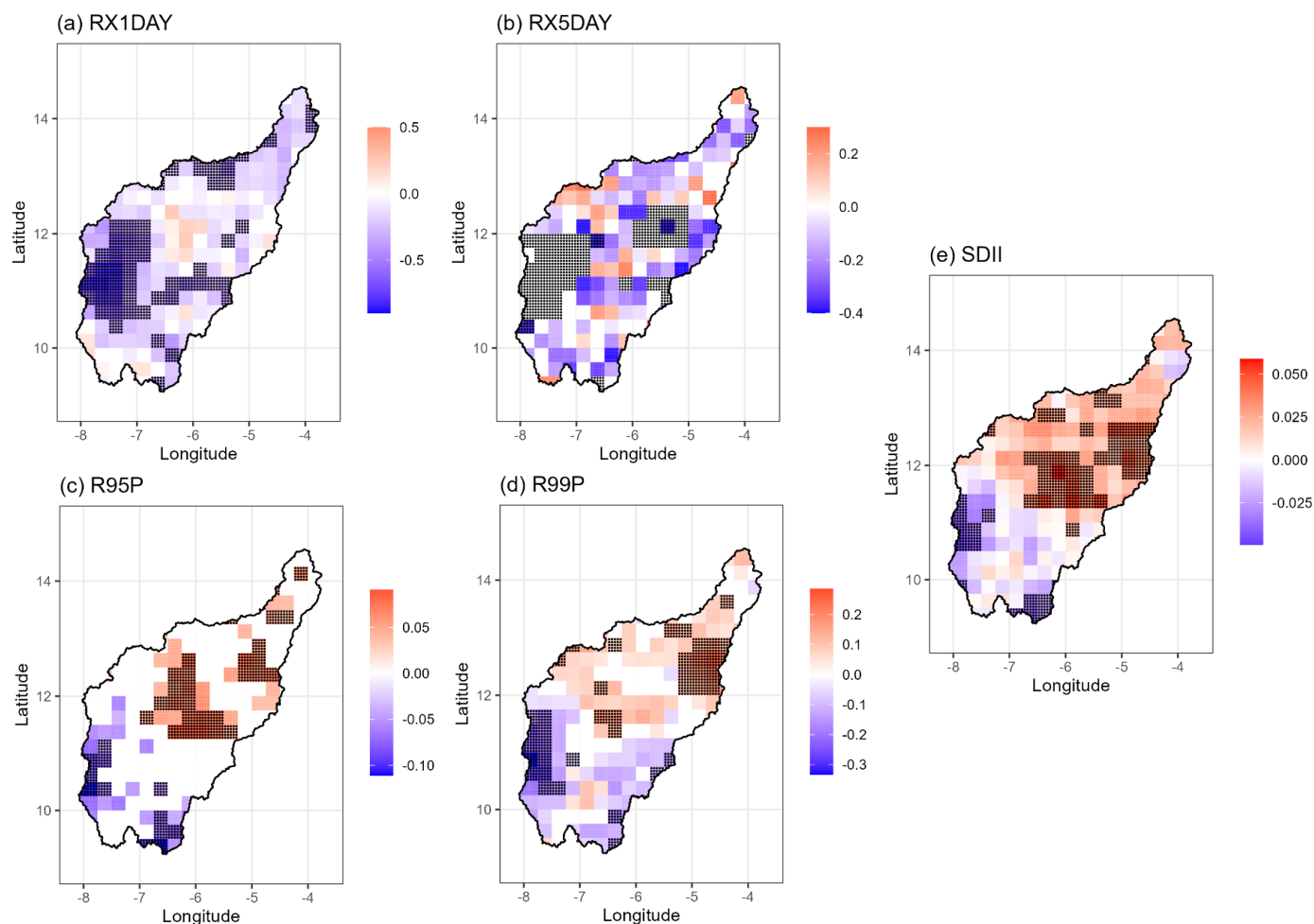


**Figure 5.** Sen's slope and trends for the BRB from 1991 to 2020: (a) RX1DAY, (b) RX5DAY, (c) R95P, (d) R99P, and (e) SDII. Black dots indicate statistically significant trends ( $p < 0.05$ ), showing the spatial patterns of changes in extreme rainfall indices across the basin.

### 3.4. Interannual Variation and Trends in Extreme Rainfall Indices

The interannual trends of the extreme rainfall indices in the BRB from 1991 to 2020 demonstrate considerable variability over time and across regions (Figure 6). The RX5DAY index shows a significant decline (Sen's slope =  $-0.15$  mm/year,  $p < 0.01$ ), particularly after 2000, indicating a reduction in prolonged heavy rainfall events that are typically associated with flooding. This trend suggests potential implications for flood risk mitigation but also raises concerns about shifts in the rainfall distribution over shorter durations. Similarly, the RX1DAY index highlights a decline (Sen's slope =  $-0.2$  mm/year,  $p < 0.01$ ), particularly after 2012, reinforcing the reduction in extreme rainfall intensities in some regions. Conversely, the R99P index displays a significant upward trend (Sen's slope =  $0.07$  mm/year,  $p < 0.001$ ), pointing to an increase in extreme rainfall events, especially in the northeastern parts of the basin. These results align with broader regional observations, such as those in [31], which reported increasing rainfall extremes across West Africa. The SDII index shows a weak

positive trend (Sen’s slope = 0.008 mm/day/year), indicating only slight changes in the rainfall intensification. Meanwhile, the R95P index, representing very wet days, shows no significant trend (Table 3), suggesting that the frequency of moderately extreme rainfall events has remained stable.

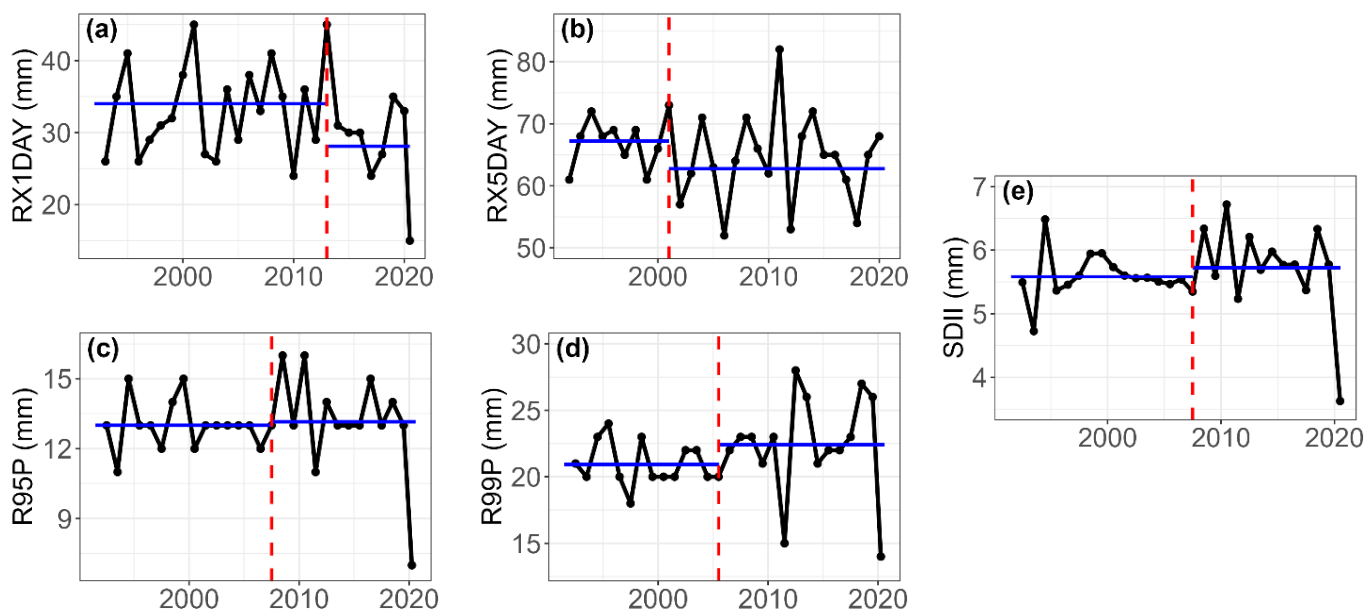


**Figure 6.** Breakpoint results for extreme precipitation over the BRB: (a) RX1DAY, (b) RX5DAY, (c) R95P, (d) R99P and (e) SDII.

**Table 3.** Modification of the Mann–Kendall test and Sen’s slope estimation from 1991 to 2020.

Indices	<i>p</i> -Value	Zc	Sen’s Slope (mm/Year)	Tau	Var(s)	Units
R95P	$11 \times 10^{-2}$	0.67	0	0.08	500.15	mm/year
R99P	$17 \times 10^{-5}$	1.18	0.07	0.15	300.42	mm/year
SDII	$43 \times 10^{-3}$	0.98	0.008	0.13	739.44	mm/year
RX1DAY	$10^{-3}$	−1.14	−0.2	−0.15	382.43	mm/year
RX5DAY	$11 \times 10^{-3}$	−1.18	−0.15	−0.15	680.5	mm/year

The breakpoints in these indices further highlight structural changes in the rainfall patterns (Figure 6). The RX1DAY index shows a marked decline after 2012, while the R99P and SDII indices indicate shifts around 2005 and 2007, respectively (Table 4). These breakpoints reflect changes in the rainfall dynamics that may be linked to broader regional climatic shifts, as noted in [12].

**Table 4.** Shifts in the extreme precipitation indices in the BRB during the period 1991–2020.

Index	<i>p</i> -Value	Breakpoint
R95p	1	2007
R99p	0.4229	2005
SDII	0.487	2007
RX1DAY	0.66	2012
RX5DAY	0.68	2000

These findings illustrate the complex nature of hydroclimatic variability in the BRB. Southern regions are experiencing reduced extreme rainfall events, while the northeastern areas face increased risks of intense rainfall and flooding.

### 3.5. Analysis of Extreme Flow Characteristics

#### 3.5.1. Interannual Variation in Discharge

Figure 7 provides insight into the fluctuations in water availability across the BRB from 1991 to 2020. The SFI effectively highlights periods of hydrological surplus and deficit, which is critical for understanding the basin's response to climatic and hydrological changes. Between 1991 and 2000, the BRB experienced multiple years of below-average discharge, as indicated by the prevalence of negative SFI values. This period reflects prolonged hydrological deficits, which align with the region's well-documented droughts during the 1990s. The deficits observed are consistent with the findings in [12], which reported significant reductions in river flows during this time due to declining rainfall. From 2001 onwards, there is a noticeable shift, with the more frequent positive SFI values reflecting above-average discharge. These findings align with broader trends in West Africa, where a partial recovery of rainfall has been observed since the late 1990s, as documented in [6]. The alternating periods of wet and dry years, especially the shifts between surplus and deficit conditions post-2010, underscore the basin's vulnerability to climatic variability.

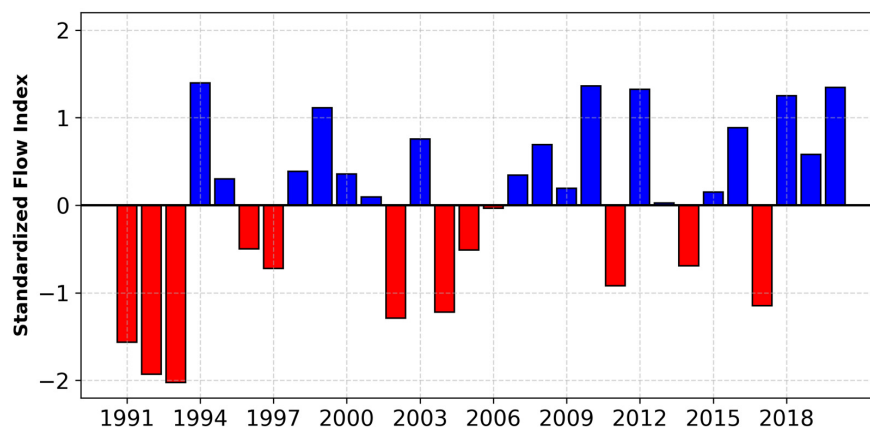


Figure 7. Standardized flow index over the BRB (1991–2020).

#### 3.5.2. Trends and Interannual Variability of Extreme Flows

The trends and interannual variability of extreme flows in the BRB from 1991 to 2020 reveal significant changes in high-flow conditions, as shown in Table 5. The analysis of indices such as the Q95P, Q99P and Qmax highlights upward trends across all three metrics, suggesting an intensification of extreme flow events over the study period. The Q95P index exhibits a significant positive trend (Sen's slope =  $19.75 \text{ m}^3/\text{s}/\text{year}$ ,  $p < 0.001$ ), indicating an increase in moderately extreme flows. Similarly, the Q99P index shows a significant rise (Sen's slope =  $21.04 \text{ m}^3/\text{s}/\text{year}$ ,  $p < 0.001$ ). This suggests a growing frequency of extreme flood conditions, which may pose heightened risks of flooding in the basin. The peak discharge, represented by the Qmax index, also demonstrates a significant upward trend (Sen's slope =  $20.92 \text{ m}^3/\text{s}/\text{year}$ ,  $p < 0.001$ ). This trend points to an intensification of the maximum river flows over time, consistent with the increasing variability of extreme flow conditions observed in the basin. The rising trends in all the indices underscore a pattern of hydrological intensification, characterized by increased flow extremes. When compared with historical discharge records and neighboring basins, these recent increases in the Q95P and Q99P are notably larger than past norms, highlighting a broader regional intensification of high-flow conditions [22,32].

**Table 5.** Sen’s slope and modified Mann–Kendall test on the extreme flow for the 1991 to 2020 period.

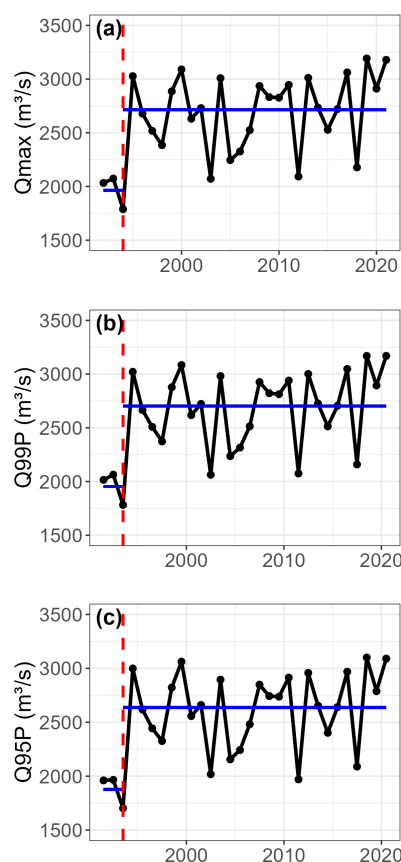
Indices	<i>p</i> -Value	Zc	Sen’s Slope	Tau	Var(s)	Units
Q95P	$24 \times 10^{-9}$	2.12	19.75	0.28	494.27	m <sup>3</sup> /s/year
Q99P	$68 \times 10^{-10}$	2.35	21.04	0.3	518	m <sup>3</sup> /s/year
Qmax	$25 \times 10^{-10}$	2.35	20.92	0.3	490	m <sup>3</sup> /s/year

### 3.5.3. Breakpoint Detection on the Trends of Extreme Flows

The analysis of the breakpoints for the extreme flow indices in the BRB identifies 1993 as an important year for significant changes in the hydrological regime. Both Pettitt’s test and the SNHT consistently detect this shift across all the indices, as shown in Table 6. The Q95P and Q99P indices, which represent high-flow and very-high-flow days, exhibit statistically significant breakpoints ( $p < 0.05$ ) in 1993. This indicates a noticeable increase in extreme flow events after this year, as reflected in Figure 8. Similarly, the Qmax index, representing the peak discharge, also shows a breakpoint in 1993, signaling a transition toward higher maximum flows. These results suggest that 1993 marks a turning point in the basin’s flow patterns, potentially due to climatic variability or environmental changes.

**Table 6.** Breakpoints related to the extreme flow indices (1991–2020).

Indices	Pettitt’s Test		SNHT	
	<i>p</i> -Value	Breakpoint	<i>p</i> -Value	Breakpoint
Q95p	0.013	1993	0.013	1993
Q99p	0.042	1993	0.0166	1993
Qmax	0.042	1993	0.139	1993

**Figure 8.** Breakpoint results for the extreme flows over the BRB (1991–2020): (a) Qmax, (b) Q99P and (c) Q95P.

## 4. Discussion

This study provides a detailed analysis of the extreme rainfall trends in the BRB from 1991 to 2020, highlighting the significant spatial and temporal variability in the rainfall indices. These findings align with broader regional and global patterns of hydroclimatic variability driven by climate change. For instance, the decline in the RX5DAY and RX1DAY indices, particularly after 2012, parallels trends observed in other semi-arid regions, such as the Sahel, where reduced prolonged rainfall events have impacted agricultural productivity and water availability [33]. Conversely, the increase in the R99P and SDII, indicating intensified short-duration rainfall, mirrors findings from basins such as the Senegal River Basin and the Ganges, where extreme rainfall events have become more frequent due to shifting climatic regimes [34,35]. The breakpoints identified (e.g., 2000 for the RX5DAY and 1993 for the extreme flows) further highlight structural changes in rainfall dynamics that may be linked to global climate drivers, such as the El Niño–Southern Oscillation (ENSO) [36].

The 1993 breakpoint in the extreme flows (Q95P, Q99P, and Qmax) may reflect broader climate regime shifts linked to large-scale ocean–atmosphere interactions, such as changes in Atlantic sea surface temperatures or ENSO cycles, which have been shown to alter precipitation patterns in West African river basins [33]. From a management perspective, recognizing this hydrological turning point underscores the need for adaptive measures such as floodplain zoning and infrastructural investments to mitigate heightened flood risks and bolster water security in the BRB [37].

These shifts present challenges for water resource management in the BRB. The rise in the R99P underscores the need for improved flood risk management in northeastern regions, including the construction of retention basins and enhanced floodplain zoning. Meanwhile, the declining RX5DAY trends in southern areas call for adaptive strategies to sustain rain-fed agriculture, such as efficient irrigation systems and water conservation measures [38,39]. Methodologically, this study leveraged the modified Mann–Kendall test to ensure reliable trend detection, accounting for autocorrelation. However, limitations in the satellite-derived CHIRPS data highlight the need to integrate ground-based observations in future research to capture localized extremes more accurately [40].

The results of this study provide a valuable framework for policymakers to develop climate adaptation strategies, balancing flood mitigation with water resource sustainability. Further cross-basin comparisons, particularly with the Senegal and Nile Basins, could enhance regional adaptation efforts.

## 5. Conclusions

The BRB has experienced significant hydroclimatic variability from 1991 to 2020, characterized by significant shifts in rainfall patterns and river discharge. Southern regions experienced reduced prolonged rainfall events, while northeastern regions faced intensified short-duration rainfall. These findings underscore the need for localized water resource management strategies tailored to these distinct regional patterns. Methodologically, the use of the modified Mann–Kendall test provided a robust trend analysis by addressing the autocorrelation in the time series data. This approach ensures reliable identification of shifts, such as the 1993 breakpoint for the river discharge and the 2000 breakpoint for the RX5DAY, which reflect broader climatic drivers like the El Niño–Southern Oscillation (ENSO). Comparing these trends to other semi-arid basins, such as the Senegal and Niger, highlights the BRB's heightened vulnerability to hydroclimatic extremes. In terms of the river discharge, indices such as the Q95P, Q99P and Qmax (peak discharge) all demonstrated significant positive trends, indicating an intensification of extreme flow events over the study period. These outcomes align with broader regional studies that project substan-

tial decreases in potential water availability across major West African river basins due to climate change [1,41,42]. Additionally, our research indicates that future water resource developments in the BRB will be significantly impacted by climate change, pointing out the need for adaptive management strategies.

The observed trends in the BRB highlight the necessity of adaptive water resource management strategies that can effectively address both the reduction in heavy rainfall events and the intensification of extreme flow events. Implementing such strategies is crucial to mitigate the impacts of climate variability and ensure sustainable water availability for agriculture, fisheries, and livelihoods in the region.

**Author Contributions:** Conceptualization, F.K. and F.K.G.; methodology, F.K. and A.N.; software, F.K., F.K.G. and A.N.; writing—original draft preparation, F.K.; writing—review and editing, F.K., F.K.G. and O.M.G.M.; visualization, F.K. and F.K.G.; supervision, F.K.G. All authors have read and agreed to the published version of the manuscript.

**Funding:** This paper is part of a doctoral research initiative, generously funded by the German Federal Ministry of Education and Research (BMBF) through the West Africa Science Center of Climate Change and Adapted Land Use (WASCAL).

**Data Availability Statement:** The materials used for this article will be made available by the authors on request.

**Acknowledgments:** This research is part of a PhD study conducted under the auspices of the West African Science Service Center on Climate Change and Adapted Land Use (WASCAL) program.

**Conflicts of Interest:** The authors declare no conflicts of interest.

## References

1. Sylla, M.B.; Faye, A.; Klutse, N.A.B.; Dimobe, K. Projected Increased Risk of Water Deficit over Major West African River Basins Under Future Climates. *Clim. Chang.* **2018**, *151*, 247–258. [[CrossRef](#)]
2. Oyerinde, G.T.; Fademi, I.O.; Denton, O.A. Modeling Runoff with Satellite-Based Rainfall Estimates in the Niger Basin. *Cogent Food Agric.* **2017**, *3*, 1363340. [[CrossRef](#)]
3. Roudier, P.; Mahe, G. Study of Water Stress and Droughts with Indicators Using Daily Data on the Bani River (Niger Basin, Mali). *Int. J. Climatol.* **2010**, *30*, 1689–1705. [[CrossRef](#)]
4. Dos Santos, M.R.W. Water Cooperation Within West Africa’s Major Transboundary River Basins. *Reg. Cohes.* **2023**, *13*, 25–52. [[CrossRef](#)]
5. Descroix, L.; Genthon, P.; Amogu, O.; Rajot, J.-L.; Sighomnou, D.; Vauclin, M. Change in Sahelian Rivers Hydrograph: The Case of Recent Red Floods of the Niger River in the Niamey Region. *Glob. Planet. Chang.* **2012**, *98–99*, 18–30. [[CrossRef](#)]
6. Ndiaye, A.; Mbaye, M.L.; Arnault, J.; Camara, M.; Lawin, A.E. Characterization of Extreme Rainfall and River Discharge over the Senegal River Basin from 1982 to 2021. *Hydrology* **2023**, *10*, 204. [[CrossRef](#)]
7. Bodian, A.; Diop, L.; Panthou, G.; Dacosta, H.; Deme, A.; Dezetter, A.; Ndiaye, P.M.; Diouf, I.; Vischel, T. Recent Trend in Hydroclimatic Conditions in the Senegal River Basin. *Water* **2020**, *12*, 436. [[CrossRef](#)]
8. Louvet, S.; Paturel, J.E.; Mahé, G.; Rouché, N.; Koité, M. Comparison of the Spatiotemporal Variability of Rainfall from Four Different Interpolation Methods and Impact on the Result of GR2M Hydrological Modeling—Case of Bani River in Mali, West Africa. *Theor. Appl. Climatol.* **2016**, *123*, 303–319. [[CrossRef](#)]
9. Mahe, G. Surface/Groundwater Interactions in the Bani and Nakambe Rivers, Tributaries of the Niger and Volta Basins, West Africa. *Hydrol. Sci. J.* **2009**, *54*, 704–712. [[CrossRef](#)]
10. Dembélé, M.; Zwart, S.J. Evaluation and Comparison of Satellite-Based Rainfall Products in Burkina Faso, West Africa. *Int. J. Remote Sens.* **2016**, *37*, 3995–4014. [[CrossRef](#)]
11. Diop, L.; Samadianfard, S.; Bodian, A.; Yaseen, Z.M.; Ghorbani, M.A.; Salimi, H. Annual Rainfall Forecasting Using Hybrid Artificial Intelligence Model: Integration of Multilayer Perceptron with Whale Optimization Algorithm. *Water Resour. Manag.* **2020**, *34*, 733–746. [[CrossRef](#)]
12. Chaibou Begou, J.; Jomaa, S.; Benabdallah, S.; Bazie, P.; Afouda, A.; Rode, M. Multi-Site Validation of the SWAT Model on the Bani Catchment: Model Performance and Predictive Uncertainty. *Water* **2016**, *8*, 178. [[CrossRef](#)]
13. Ruelland, D.; Ardoin-Bardin, S.; Collet, L.; Roucou, P. How Could Hydro-Climatic Conditions Evolve in the Long Term in West Africa? The Case Study of the Bani River Catchment. *Hydro-Climatol. Var. Chang.* **2011**, *344*, 195–201.

14. Rameshwaran, P.; Bell, V.A.; Davies, H.N.; Kay, A.L. How Might Climate Change Affect River Flows Across West Africa? *Clim. Chang.* **2021**, *169*, 21. [[CrossRef](#)]
15. Roudier, P.; Ducharme, A.; Feyen, L. Climate Change Impacts on Runoff in West Africa: A Review. *Hydrol. Earth Syst. Sci.* **2014**, *18*, 2789–2801. [[CrossRef](#)]
16. Mahe, G.; Lienou, G.; Descroix, L.; Bamba, F.; Paturel, J.E.; Laraque, A.; Meddi, M.; Habaieb, H.; Adeaga, O.; Dieulin, C.; et al. The Rivers of Africa: Witness of Climate Change and Human Impact on the Environment. *Hydrol. Process.* **2013**, *27*, 2105–2114. [[CrossRef](#)]
17. HOUNGNIPO, M.C.M.; MINOUNGOU, B.; TRAORE, S.B.; MAIDMENT, R.I.; ALHASSANE, A.; ALI, A. Validation of High-Resolution Satellite Precipitation Products over West Africa for Rainfall Monitoring and Early Warning. *Front. Clim.* **2023**, *5*, 1185754. [[CrossRef](#)]
18. De Luca, P.; Messori, G.; Wilby, R.L.; Mazzoleni, M.; Di Baldassarre, G. Concurrent Wet and Dry Hydrological Extremes at the Global Scale. *Earth Syst. Dyn.* **2020**, *11*, 251–266. [[CrossRef](#)]
19. Hamed, K.H.; Ramachandra Rao, A. A Modified Mann-Kendall Trend Test for Autocorrelated Data. *J. Hydrol.* **1998**, *204*, 182–196. [[CrossRef](#)]
20. Yue, S.; Wang, C.Y. Applicability of Prewhitening to Eliminate the Influence of Serial Correlation on the Mann-Kendall Test. *Water Resour. Res.* **2002**, *38*, 4-1–4-7. [[CrossRef](#)]
21. Ehsanzadeh, E.; Adamowski, K. Trends in Timing of Low Stream Flows in Canada: Impact of Autocorrelation and Long-term Persistence. *Hydrol. Process.* **2010**, *24*, 970–980. [[CrossRef](#)]
22. Kundzewicz, Z.W.; Robson, A.J. Change Detection in Hydrological Records—A Review of the Methodology/Revue Méthodologique de La Détection de Changements Dans Les Chroniques Hydrologiques. *Hydrol. Sci. J.* **2004**, *49*, 7–19. [[CrossRef](#)]
23. Hamitouche, Y.; Zeroual, A.; Meddi, M.; Assani, A.A.; Alkama, R.; Şen, Z.; Zhang, X. Projected Changes in Extreme Precipitation Patterns across Algerian Sub-Regions. *Water* **2024**, *16*, 1353. [[CrossRef](#)]
24. Burn, D.H.; Hag Elnur, M.A. Detection of Hydrologic Trends and Variability. *J. Hydrol.* **2002**, *255*, 107–122. [[CrossRef](#)]
25. Serinaldi, F.; Kilsby, C.G. The Importance of Prewhitening in Change Point Analysis Under Persistence. *Stoch. Environ. Res. Risk Assess.* **2016**, *30*, 763–777. [[CrossRef](#)]
26. Sang, Y.-F.; Wang, Z.; Liu, C. Comparison of the MK Test and EMD Method for Trend Identification in Hydrological Time Series. *J. Hydrol.* **2014**, *510*, 293–298. [[CrossRef](#)]
27. Pettitt, A.N. A Non-Parametric Approach to the Change-Point Problem. *Appl. Stat.* **1979**, *28*, 126. [[CrossRef](#)]
28. Khaliq, M.N.; Ouarda, T.B.M.J.; Gachon, P.; Sushama, L.; St-Hilaire, A. Identification of Hydrological Trends in the Presence of Serial and Cross Correlations: A Review of Selected Methods and Their Application to Annual Flow Regimes of Canadian Rivers. *J. Hydrol.* **2009**, *368*, 117–130. [[CrossRef](#)]
29. Funk, C.; Peterson, P.; Landsfeld, M.; Pedreros, D.; Verdin, J.; Shukla, S.; Husak, G.; Rowland, J.; Harrison, L.; Hoell, A.; et al. The Climate Hazards Infrared Precipitation with Stations—A New Environmental Record for Monitoring Extremes. *Sci. Data* **2015**, *2*, 150066. [[CrossRef](#)] [[PubMed](#)]
30. Ogunrinde, A.T.; Oguntunde, P.G.; Akinwumiju, A.S.; Fasinmirin, J.T. Evaluation of the Impact of Climate Change on the Characteristics of Drought in Sahel Region of Nigeria: 1971–2060. *Afr. Geogr. Rev.* **2021**, *40*, 192–210. [[CrossRef](#)]
31. Quenum, G.M.L.D.; Nkrumah, F.; Klutse, N.A.B.; Sylla, M.B. Spatiotemporal Changes in Temperature and Precipitation in West Africa. Part I: Analysis with the CMIP6 Historical Dataset. *Water* **2021**, *13*, 3506. [[CrossRef](#)]
32. Intergovernmental Panel on Climate Change (IPCC) *Climate Change 2021—The Physical Science Basis: Working Group I Contribution to the Sixth Assessment Report of the Intergovernmental Panel on Climate Change*, 1st ed.; Cambridge University Press: Cambridge, UK, 2023; ISBN 978-1-00-915789-6.
33. Nicholson, S.E. The West African Sahel: A Review of Recent Studies on the Rainfall Regime and Its Interannual Variability. *ISRN Meteorol.* **2013**, *2013*, 1–32. [[CrossRef](#)]
34. Sylla, M.B.; Giorgi, F.; Pal, J.S.; Gibba, P.; Kebe, I.; Nikiema, M. Projected Changes in the Annual Cycle of High-Intensity Precipitation Events over West Africa for the Late Twenty-First Century\*. *J. Clim.* **2015**, *28*, 6475–6488. [[CrossRef](#)]
35. Mishra, A.K.; Singh, V.P. Drought Modeling—A Review. *J. Hydrol.* **2011**, *403*, 157–175. [[CrossRef](#)]
36. Ward, P.J.; Jongman, B.; Kumm, M.; Dettinger, M.D.; Sperna Weiland, F.C.; Winsemius, H.C. Strong Influence of El Niño Southern Oscillation on Flood Risk Around the World. *Proc. Natl. Acad. Sci. USA* **2014**, *111*, 15659–15664. [[CrossRef](#)] [[PubMed](#)]
37. Di Baldassarre, G.; Sivapalan, M.; Rusca, M.; Cudennec, C.; Garcia, M.; Kreibich, H.; Konar, M.; Mondino, E.; Mård, J.; Pande, S.; et al. Sociohydrology: Scientific Challenges in Addressing the Sustainable Development Goals. *Water Resour. Res.* **2019**, *55*, 6327–6355. [[CrossRef](#)] [[PubMed](#)]
38. Biasutti, M. Rainfall Trends in the African Sahel: Characteristics, Processes, and Causes. *WIREs Clim. Chang.* **2019**, *10*, e591. [[CrossRef](#)] [[PubMed](#)]
39. Sultan, B.; Gaetani, M. Agriculture in West Africa in the Twenty-First Century: Climate Change and Impacts Scenarios, and Potential for Adaptation. *Front. Plant Sci.* **2016**, *7*, 1262. [[CrossRef](#)] [[PubMed](#)]

40. Dinku, T.; Ceccato, P.; Cressman, K.; Connor, S.J. Evaluating Detection Skills of Satellite Rainfall Estimates over Desert Locust Recession Regions. *J. Appl. Meteorol. Climatol.* **2010**, *49*, 1322–1332. [[CrossRef](#)]
41. Carr, T.W.; Mkuhlani, S.; Segnon, A.C.; Ali, Z.; Zougmore, R.; Dangour, A.D.; Green, R.; Scheelbeek, P. Climate Change Impacts and Adaptation Strategies for Crops in West Africa: A Systematic Review. *Environ. Res. Lett.* **2022**, *17*, 053001. [[CrossRef](#)]
42. Fofana, M.; Adoukpe, J.; Larbi, I.; Hounkpe, J.; Djan'na Koubodana, H.; Toure, A.; Bokar, H.; Dotse, S.-Q.; Limantol, A.M. Urban Flash Flood and Extreme Rainfall Events Trend Analysis in Bamako, Mali. *Environ. Chall.* **2022**, *6*, 100449. [[CrossRef](#)]

**Disclaimer/Publisher's Note:** The statements, opinions and data contained in all publications are solely those of the individual author(s) and contributor(s) and not of MDPI and/or the editor(s). MDPI and/or the editor(s) disclaim responsibility for any injury to people or property resulting from any ideas, methods, instructions or products referred to in the content.